Food Chemistry 434 (2024) 137442

Contents lists available at ScienceDirect

Food Chemistry

journal homepage: www.elsevier.com/locate/foodchem

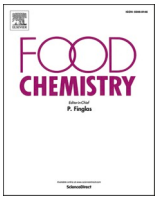

Effects of microwave processing in comparison to sous vide cooking on meat quality, protein structural changes, and in vitro digestibility

Mariero Gawat [a,b], Mike Boland [b], Jim Chen [a], Jaspreet Singh [a,b], Lovedeep Kaur [a,b,*]

[a] School of Food and Advanced Technology, Massey University, 4442 Palmerston North, New Zealand
[b] Riddet Institute, Massey University, 4442 Palmerston North, New Zealand

ARTICLE INFO

Keywords:
FTIR spectroscopy
Protein aggregation
Protein surface hydrophobicity
Meat ultrastructure
Microwave processing
Meat digestion

ABSTRACT

This study investigated the effect of industrial microwave (MW) processing, and sous vide (SV) on goat and lamb *biceps femoris*, where samples were cooked to the same tenderness. The cooked meat quality and ultrastructure were analyzed along with determining the protein surface hydrophobicity, particle size distribution, secondary structure, and protein digestibility. MW-processing resulted in higher cooking loss and more ultrastructural damage than SV and also induced higher myofibrillar protein surface hydrophobicity. Both processes caused a significant increase ($p < 0.05$) in the β-sheet and an increase in the random coils with a reduction ($p < 0.05$) in α-helix and β-turns. Both processes led to different protein hydrolysis patterns (observed through SDS-PAGE), but overall free amino N release after digestion was not significantly different among them. The results suggest that MW and SV modify meat protein structure differently, but with the same meat tenderness level, these processes can lead to similar overall protein digestibility.

1. Introduction

Thermal treatment is widely employed for cooking meat. Apart from making the food appealing and safe to eat, the thermal processes may alter the composition and nutritional quality of food, depending on the severity of the process (Astruc, 2014). Microwave (MW) heating has gained much attention in recent years because of the development of microwave-assisted thermal processing (MATS) that aims to produce ready-to-eat products on an industrial scale via a fast heating process (Soni et al., 2020). Additionally, MW cooking has been valuable in reducing food preparation time. The mechanism of MW heating uses the polarization effect of electromagnetic radiation that transforms electromagnetic energy into thermal energy; it relies heavily on the food dielectric property that affects the degree of heat generated within the system (Soni et al., 2020). However, the effect of MW heating and its nonthermal mechanism on protein secondary structure has been linked to the nutritive quality of meat proteins (Calabrò & Magazù, 2014, 2020), and research on the digestibility and utilization of MW-cooked proteins was raised to be further investigated (Cai et al., 2018).

In contrast to MW heating, sous vide (SV) cooking is a slow process involving long-time low-temperature heat treatment with precise temperature control. This process has become popular since it is thought to be less intensive and can also be used to prolong the shelf-life of minimally processed food and to tenderize tough meat. The nutritive value of SV processed meat in terms of protein digestibility has been widely studied (Bhat et al., 2020; Chian et al., 2019). It was reported that SV has no negative impact on the myofibrillar protein profile of meat and significantly improves the in-vitro digestion of proteins (Bhat et al., 2020). Unlike MW, SV processing was described as a novel process that produces superior-quality cooked meat.

The nutritional value of meat is determined by how proteins can be efficiently broken-down into shorter peptides and free amino acids by digestive enzymes to be used by the body. In food processing, various thermal processing methods exert different effects on protein digestibility. Heat treatments can enhance the accessibility of pepsin to cleavage sites by denaturing proteins and breaking structures (Astruc, 2014; Bax et al., 2012). However, heating can also promote significant protein aggregation that hinders efficient enzymatic hydrolysis, thereby reducing the digestibility of proteins (Sante-Lhoutellier et al., 2007). At present, the studies on the impact of MW cooking on meat proteins are mostly limited only to the effect of MW on protein structural changes (Cai et al., 2018; Calabrò & Magazù, 2020; Cao et al., 2019), and recent digestibility studies were carried out for gluten (Xiang et al., 2020) and pea (Sun et al., 2020), and shrimp (Dong et al., 2021). However, based

* Corresponding author at: School of Food and Advanced Technology, Massey University, 4442 Palmerston North, New Zealand.
E-mail address: L.Kaur@massey.ac.nz (L. Kaur).

https://doi.org/10.1016/j.foodchem.2023.137442
Received 20 March 2023; Received in revised form 6 August 2023; Accepted 7 September 2023
Available online 9 September 2023

on our knowledge, the direct impact of the MW process on red meat structural changes and its effect on protein digestibility has not been demonstrated, specifically for lamb and goat meat. We aim to understand the impact of MW compared to a known process that is practically used in cooking meat, such as SV. Moreover, the meat samples from two different species, goat meat, and lamb, were compared to further understand how the selected processes can affect meat samples that require longer cooking time and are popular meat options for stews and curries. The *biceps femoris* part of lamb and goat meat are from tough cuts and is considered a less tender meat that requires longer cooking methods. Hence the use of SV as a common cooking technique was chosen.

Therefore, this study was designed to determine the effect of MW heating in a real meat system, which involves high-temperature intensive processing, versus the SV process, which requires a long-time and low-temperature process, on the meat quality and ultrastructural changes in meat. More importantly, this study aims to evaluate the effect of MW and SV on the protein structural changes, such as particle size and distribution and protein surface hydrophobicity, to describe the denaturation and aggregation behavior of the proteins that plays a significant role in the digestibility of proteins. The protein secondary structure was also examined since its alteration during microwaving has been linked to causing low protein value for meat (Calabrò & Magazù, 2020). Furthermore, this paper aims to provide direct consequences of MW processing on meat protein digestibility. We hypothesized that MW processing would lead to significant structural modification of meat proteins that might reduce the digestibility of proteins compared to the milder effects of SV cooking at 60 °C.

2. Materials and methods

2.1. Meat samples

The *biceps femoris* (BF) muscles of lamb and goat meat were used in this study. A total of 6 animals of each species were used in the study. The lamb samples were purchased as a bone-in lamb leg cut, supplied by Wilson Hellaby (Auckland, New Zealand), and purchased from The Mad Butcher, Palmerston North, New Zealand. The lamb was aged for 10 days at 4 °C after slaughter, and its average pH was 5.34, measured by an insertion electrode (Mettler-Toledo Inlab 427). The goat meat samples were dissected whole BF from female Boer cross goats supplied by Shingle Creek Chevon (Central Otago, New Zealand) with 15 kg, an average empty body weight, and a fat score of 3 to 4 (girth rib (GR). The goat meat samples were wet-aged for four days at 4 °C and had a pH of 5.18. The lamb and goat meat BF muscles were dissected from the whole leg cut, and the epimysial sheath was removed. From both ends of each BF muscle, approximately 50 g was taken where a portion was immediately used for color analysis. In contrast, the remaining samples used for color analysis were minced and stored at −80 °C for proximate and protein structure analysis. The remaining large portion of the meat sample, with an average weight of 176 ± 5 g and 165 ± 5 g for lamb and goat meat samples, respectively, were prepared for processing. Supplementary Fig. 1 shows the sampling procedure on *biceps femoris* muscles.

2.2. Sample packaging

For each sample, a cylindrical PicoVacQ temperature sensor and MI-Orion probe (TMI-USA, Inc., VA, USA) were inserted in the BF muscle for temperature monitoring. Then the meat was vacuum-packed in BNB1 vacuum pouches (Cryovac, Hamilton, New Zealand) and sealed (0.023 MPa) using a Multivac C200 vacuum sealer (Multivac NZ Ltd, Auckland, New Zealand). These vacuum pouches are the designated packaging for the MW equipment. Packed samples are shown in Supplementary Fig. 2.

2.3. Sample processing

2.3.1. Microwave cooking

The MW processing was done using coaxially induced microwave pasteurization and sterilization (CiMPAS) equipment manufactured by Meyer Burger Germany GmbH (Hohenstein-Ernstthal, Germany) with the industrial microwave parts manufactured by MUEGGE GmbH (Reichelsheim, Germany). This equipment used industrial MW heating applied at 915 MHz and operated at 30 kW. The MW process was chosen after a series of preliminary experiments; prolonged MW exposure led to overcooked meat (very dry and brittle), and shorter processes led to low internal meat temperature.

The vacuum-packed samples were loaded in a tray, placed inside the heating chamber under pressure at 0.25 MPa, and flushed with water. The meat was exposed to the microwave for four consecutive passes at 100 cm/min speed. The CiMPAS enables efficient heat penetration since MW energy is emitted from above and below the food. After MW exposure, 60 °C water was flushed to reduce the temperature, and the process was stopped after 20 min holding time. The internal temperature profile of the meat samples was measured using the TMI probes inserted in the middle of the meat samples. The reported temperature was based on the corrected temperature using fiber optics. Overall, MW exposure led to an approximately 10 °C/min increase in temperature throughout the sample. By the end of the process, the maximum average temperature of the core reached 104.7 °C for goat meat and 117.8 °C for lamb. A sample temperature profile of the whole MW process is shown in Supplementary Fig. 3. After the entire process, the pouches were immediately immersed in an ice bath. Although the MW equipment involved elevated pressure, the main physicochemical changes undergone by the MW processed meat are attributed to the effects of high temperature induced by MW heating. The pressure of the chamber was only 0.25 MPa compared to the industrial HPP equipment that uses 100–900 MPa.

2.3.2. Sous vide cooking

BF muscle was prepared and vacuum-packed for SV cooking the same way as samples used for MW processing. Preliminary experiments were conducted to determine the SV cooking time that can provide the same level of tenderness as that of the MW meat. Packed meat was subjected to SV cooking at 60 °C using various cooking times (6, 8, 10, and 12 h). A temperature of 60 °C was selected since it is the water temperature in the MW chamber, a widely used temperature for SV, and is an approved temperature for cooking meat in New Zealand according to Ministry for Primary Industry guidelines. The SV cooking of meat at 60 °C for 9 h gave the same tenderness as meat processed using MW. The tenderness values achieved by MW and SV processing using lamb and goat meat are in the acceptable tenderness value range (~<43 N) (Destefanis et al., 2008).

2.4. Processed meat quality assessment

2.4.1. Texture

The instrumental texture of the MW and SV samples was analyzed using a TA.XT plus texture analyzer (Stable Microsystems, Godalming, UK) fitted with a Warner-Bratzler Shear device (V-notched cutting blade, with a blade thickness of 1.1684 mm and a V-notched angle at 60°). The cooked meat was chilled overnight at 4 °C before the sample preparation and analysis. For each sample, 6 cuboids (1 cm^2 shear area) with a fiber direction parallel to the length of the sample were taken and sheared perpendicularly. The peak force was obtained using a 50 N load cell with a crosshead speed of 250 mm/min (Gawat et al., 2022).

2.4.2. Cooking loss

After cooling, the cooked SV and MW meat samples were taken from the vacuum pouch, blot dried with filter paper, and weighed. The cooking loss (%) was computed using Eq. (1).

$$\text{Cooking loss (\%)} = [(\text{raw weight} - \text{cooked weight})/\text{raw weight}] \times 100 \quad (1)$$

2.4.3. Color

The mid-section of the whole BF muscle was cut, and three sections with a thickness of 12–15 mm were taken and allowed to bloom on a tray at 4 °C for 30 min. After blooming, two locations for each cut section were randomly chosen for the analysis; six measurement points were taken for each location. A handheld Minolta Chroma Meter CR- 200 (aperture size of 3.18 cm, Konica Minolta Sensing, Inc., Japan) was used to measure lightness (L^*), redness (a^*), and yellowness (b^*), taken under D65 Illuminant and at 10° observer angle. The instrument was calibrated using a white standard plate (L* = 90.26, a* = 1.29, b* = 5.18). The chroma (color intensity, C = [a*2 + b*2]1/2) and hue angle (discoloration, HA = tan − 1 [b*/a*]) were also computed.

2.5. Meat ultrastructure

The meat ultrastructural was evaluated using Transmission Electron Microscopy (TEM) using the FEI Tecnai G^2 Spirit BioTWIN transmission electron microscope (FEI Corp., Brno-Černovice, Czech Republic). The sample collection, preparation, and staining were done following the method described by Chian et al. (2019). Then, the images were examined following the procedure outlined by Gawat et al. (2022) using the ImageJ software version 1.53a (National Institute of Health, Bethesda, MD, USA), with some modifications. Ultrastructural examination for all the treatments was carried out using one representative animal sample each for lamb and goat. A total of 10 images were examined for one sample, and 10 muscle fibers per image were randomly chosen for sarcomere length measurement.

2.6. Protein degree of aggregation

The degree of protein aggregation was measured by analyzing the particle size distribution of the myofibrillar protein. The myofibrillar protein was extracted following the method of Martinaud et al. (1997) with modifications. A 2.5 g aliquot of thawed tissue was minced and homogenized for 1 min in an Ultra-Turrax T homogenizer (Ultra-Turrax T8 Ika Labortechnik, Germany) with 25 mL of cold isolation buffer containing 150 mM NaCl, 25 mM KCl, 3 mM $MgCl_2$, 0.4 mM Pefabloc and 4 mM EDTA at pH 6.5. The collagen was eliminated by filtration on gauze. After 30 min of stirring in ice, the extract was centrifuged at 2000 × *g* for 15 min at 4 ℃. Next, the pellet was collected and washed twice with 25 mL of a 50 mM KCl and 5 mM mercaptoethanol solution at pH 6.4 and once with 25 mL of 20 mM phosphate buffer at pH 6.0. After washing, the pellet was resuspended in the phosphate buffer at pH 5.8. The protein concentration of the extracted myofibril was measured using the Bradford microplate standard assay with bovine serum albumin (BSA) as a standard; absorbance was read at 280 nm using a Synergy 2 Multi-Detection microplate reader (BioTek, USA). The myofibrillar protein isolate (MPI) was stored in a 4 °C cold room and analyzed within 24 h.

The particle diameters and size distribution were measured via static light scattering technique using the laser diffraction method, Mastersizer 2000 (Malvern Instruments, UK) (Mitra et al., 2017). The volume-weighted ($D_{4,3}$) and surface-weighted ($D_{3,2}$) mean particle diameters were computed from the particle size distributions. The absorption was set as 0.001; the dispersant used was water, and the particle refractive index used was 1.45. The measurement time was every 2 min and the temperature at 25 °C. The intensity of the scattered light was detected using a 633 nm laser with a scattering angle of 90°.

2.7. Myofibrillar protein surface hydrophobicity

The surface hydrophobicity of extracted myofibrils (as mentioned in section 2.6) was determined using bromophenol blue (BPB) sodium salt binding by the method of Chelh et al. (2006), with modifications. A 1 mL aliquot from a 5 mg/mL myofibrillar fraction was added to 200 µl of BPB solution (1 mg BPB/ml Milli-Q water) and mixed well. A control sample was prepared by adding 200 µl of BPB solution to 1 mL of 20 mM phosphate buffer at pH 6. Samples and control were kept under agitation at room temperature for 10 min and then centrifuged for 15 min at 2000 × *g* at 4 °C. The supernatant was diluted to 1/10 with phosphate buffer, and the absorbance of the resulting solution was measured at 595 nm. The myofibrillar surface hydrophobicity in terms of bound BPB was computed using Eq. (2):

$$\text{BPB bound (mg)} = 200\ \text{mg} \times [(\text{Abs control} - \text{Abs sample})/\text{Abs control}] \quad (2)$$

Abs = Absorbance at 595 nm

2.8. Fourier transform infrared (FTIR) spectroscopy

The qualitative changes in meat structure after processing were evaluated using Fourier transform infrared (FTIR) spectroscopy. The samples were first lyophilized and had a final moisture content of 6.0–6.9 %. Then, the dried samples were ground, powdered, and sieved using a 316 stainless steel mesh with a 65 µm aperture. The analysis was carried out using a Nicolet™ iS™ 5 FTIR Spectrometer (Thermo Fisher Scientific Inc., Waltham, MA, USA) with an iD7 ATR accessory (Thermo Fisher Scientific Inc., Waltham, MA, USA). The scan was conducted between 4000 and 450 cm^{-1} with a resolution of 2 cm^{-1}. The background spectrum was obtained initially and automatically subtracted from every acquisition; it was reset after scanning for 1 hr. For each sample spectrum, 32 scans were accumulated and averaged. Finally, each spectrum was baseline corrected, normalized, and averaged for qualitative interpretation of spectra.

2.8.1. Deconvolution of the amide I region

The deconvolution of the amide I region (1600 and 1700 cm^{-1}) was done for further quantitative analysis using Peakfit 4.12 software (Systat Software, Inc., CA, USA). First, each spectrum was processed for baseline correction and smoothing using a Fast Fourier Transform (FFT) filter with a smoothing length width set at 10 %. Next, peak fitting was done using the second derivative and subsequent peak fitting using the assumption of the Voigt curve (Fellows et al., 2020). Several iterations were done until the fit converged with a final fitting curve that achieved a corrected $R^2 \geq 0.99$. The resulting peaks after deconvolution were identified based on known IR spectral data for protein secondary structures. Finally, the area under each peak was evaluated against the total area and expressed as a percentage. The reported values for β-sheet and β-turns are the accumulated values of more than one peak.

2.9. In vitro protein digestibility

Simulated gastrointestinal digestion was conducted according to the guidelines of INFOGEST for static in vitro digestion (Brodkorb et al., 2019) in a double-jacketed glass reactor set-up described by Kaur et al. (2010). Digestion was carried out in triplicate for each sample.

The cooked meat sample was chopped into small pieces (~1 cm diameter). Next, a representative sample was ground using a stainless-steel coffee grinder (Model BCG200, Breville, AU) for four pulses, achieving a size of ~ 1.5 to 2 mm (Chian et al., 2019). The total crude protein content for raw and cooked samples was determined using the Kjeldahl method 984.13 (AOAC, 1990) using a FOSS Kjeltec™ 8200 analyzer (FOSS, Denmark). Eight grams of cooked meat sample, including the cooking loss, was mixed with 5.0 mL simulated salivary fluid, 1.4 mL α-amylase (10025, Sigma-Aldrich, USA) (30 U/mg), and 1.56 mL MQ water to initiate the oral phase at pH 7 ± 0.1 for 2 min. Next, the mixture had 10 mL simulated gastric fluid, 4.56 mL porcine pepsin (P7125, Sigma-Aldrich, USA) (185 U/mg) and 1.112 mL MQ water added to start the gastric phase. The pH was adjusted and

maintained at 3.0 ± 0.1 using 0.5 M HCl. Gastric digestion was carried out for 2 h. For the small-intestinal phase, the mixture was added with 15.6 mL simulated intestinal fluid, 2.096 MQ water, 10 mL pancreatin (P1750, Sigma Aldrich, USA) (27 U/mg), and 4 mL bile (B8631, Sigma-Aldrich, USA). The pH was adjusted and maintained at 7 ± 0.1 by adding NaOH (0.1 M). The digest samples were taken after 1, 10, and 120 min of gastric digestion, and pepsin activity was immediately stopped by adding Pepstatin A (abcam, UK) (200 µl/15 mL digest). Digest samples from the small-intestinal phase were taken after 10, 60, and 120 min of small-intestinal digestion, and the proteolytic enzyme activity was stopped using SIGMAFAST™ Protease inhibitor (Sigma Aldrich, USA) (2.5 mL/10 mL digest). All the digests were immediately stored at −20 °C for further analysis.

2.9.1. SDS-PAGE analysis of digests

The protein profile of each digest was evaluated using reduced-tricine-sodium dodecyl sulfate–polyacrylamide gel electrophoresis (SDS-PAGE) following the method of Kaur et al. (2010), with modifications. The digest was thawed and centrifuged at 13,000 × *g* for 2 min, and the supernatant was diluted with Milli-Q water, adjusting the volume to the desired protein concentration. The diluted digests were mixed in a 1:1 ratio with premixed tricine sample buffer (1610739, Bio-Rad Laboratories, USA) with 2 % β-mercaptoethanol (M6250, Sigma-Aldrich, USA) and then heated at 100 °C for 5 min. The electrophoresis was run using 16.5% Criterion™ Tris-Tricine Gel (Bio-Rad Laboratories Pty Ltd., New Zealand) at 125 V for 2 h, followed by fixing in fixing solution (40% methanol and 10% acetic acid) for 1 hr and staining with premixed staining solution Bio-Safe™ Coomassie Stain (Bio-Rad Laboratories Pty Ltd., New Zealand) for another hour. Afterward, the gels were rinsed and soaked with MQ water overnight, with agitation, using a shaker. The gel image was obtained using Gel Doc XR + scanning densitometer (Bio-Rad Laboratories Pty Ltd., New Zealand), and bands were analyzed using Image Lab™ software version 6.0.0 (Bio-Rad Laboratories, Inc., CA, USA).

2.9.2. Protein hydrolysis (%)

The degree of protein hydrolysis was determined by quantifying free-amino nitrogen. The digest was centrifuged for 5 min at 13,000 × g and filtered using a 0.45 µm PVDF filter, Millex ® (Merck, Germany). The gastric and small intestinal digests were diluted 1:8 with Milli-Q water at pH 3 and 7, respectively. The free amino nitrogen content of each sample was measured using the ninhydrin assay outlined by Moore (1968) using 0.2 % ninhydrin reagent (N7285, Sigma-Aldrich, USA).

2.10. Statistical analysis

Statistical analysis was performed using Minitab Version 19.2020.2.0 (Minitab Inc., State College, PA, USA). The determinations of each parameter were done in triplicate unless otherwise stated. Before analysis, a normality test was performed using the Shapiro-Wilk test, and outliers (computed using Dixon's test) were removed where applicable. The analysis of variance was determined using Minitab General Mixed Model, with processing condition as a fixed factor and the animal number as the random variable. When at least one group was statistically different, multiple comparison analysis was done using the Tukey test set at a 95 % confidence interval.

3. Results and discussion

3.1. Meat quality

The preliminary experiments using the different times for SV cooking at 60 °C resulted in varying levels of tenderness. The longer the SV time, the lower the WBSF (N) value (Data not shown). The 9 h SV was used as a reference for the study since MW-processed meat was aimed to be compared to a SV process that provides the same level of tenderness. With the given postmortem conditions of the *biceps femoris* for lamb and goat meat, the MW and SV resulted in different levels of tenderness. Expectedly, for lamb, the MW and SV processes resulted in tenderness values from 21.45 to 23 N, considered very tender (WBSF < 32.96 N) (Destefanis et al., 2008). The chosen SV process would be too intense for lamb since it resulted in very tender cooked meat. However, for the goat meat, the process resulted in WBSF values from 42.75 to 43.78 N (intermediate tenderness:42 N < WBSF < 52 N) (Destefanis et al., 2008). The intensity of the MW and SV processes used needs to be increased to achieve more acceptable tenderness values that should be below 40 N.

The cooking loss for MW samples was significantly higher than the SV samples for goat meat and lamb (Supplementary Table 1). These results agree with the literature observation that MW results in higher cooking loss than water bath processing (Wang et al., 2019). Various factors can explain the varying cooking loss between treatments. First, the different degrees of muscle fiber and connective tissue shrinkage are influenced by the temperature, where a high temperature (>100 °C) can induce a higher degree of longitudinal shrinkage resulting in greater water loss compared to the SV (Roldán et al., 2013). In this study, MW resulted in high-temperature processing (>100 °C), which causes shrinkage of myofibrils and the connective tissue network, expulsing moisture, solubilized proteins, and fats. Conversely, an SV process with low-temperature and slow heating can cause limited longitudinal shrinkage compared to higher-temperature cooking (Dominguez-Hernandez et al., 2018). The higher heating rate in MW causes a significantly higher cooking loss than slow heating in SV because high heating rate results in higher mobility of bound water (Mortensen et al., 2006). Lastly, the varying cooking loss can be explained by the length of cooking time. SV processed meat had a lower cooking loss because longer cooking results in a higher level of solubilization and gelation of collagen, which enhances the water-holding capacity of the meat matrix (Tornberg, 2005).

Both SV and MW caused a significant reduction of a* (redness) for both lamb and goat meat. Still, MW samples had a significantly lower ($p < 0.05$) redness compared to SV samples (Supplementary Table 1). The MW process gave a distinct cooked appearance, suggesting a higher degree of doneness than the SV samples. Relative to the raw sample, MW led to a higher ($p < 0.05$) pigment discoloration (hue) with significantly lower ($p < 0.05$) intensity (chroma) compared to SV. The temperature difference between SV and MW can explain the color difference in the cooked meat. Even for a short duration, the high-temperature cooking for MW resulted in a significant reduction in a* and increased L*. On the other hand, the SV cooked at 60 °C had less myoglobin denaturation. This finding agrees with observations for SV processing, where meat cooked by SV displays a more intense reddish and less brown color (García-Segovia et al., 2007). The high endpoint temperature of MW meat was sufficient to denature myoglobin, which is unstable at temperatures > 60°C (García-Segovia et al., 2007). For high temperatures, the mechanisms of the redox chemistry of myoglobin involve a reduction of the amount of deoxymyoglobin and oxymyoglobin and an increase in metmyoglobin.

3.2. Meat ultrastructure

MW processes led to changes in meat structure. Regardless of the type of meat, both processes led to an increase in Z-disk thickness, swollen coagulated mitochondrial matrix, weakening of the Z-disk and I-band junctions, and detachment of the sarcolemma from the myofibrils. Furthermore, granular aggregates in gaps between the endomysium and myofibrillar mass were seen. These observations are common changes in red meat that undergoes cooking (Chian et al., 2019; Tornberg, 2005). However, the level of the resulting ultrastructural damage varied between the two processes. Rapid MW heating resulted in significantly torn myofibrils occurring randomly between muscle fibers and along the Z-line (Fig. 1). This muscle fiber disruption was also present in SV samples but to a very low degree.

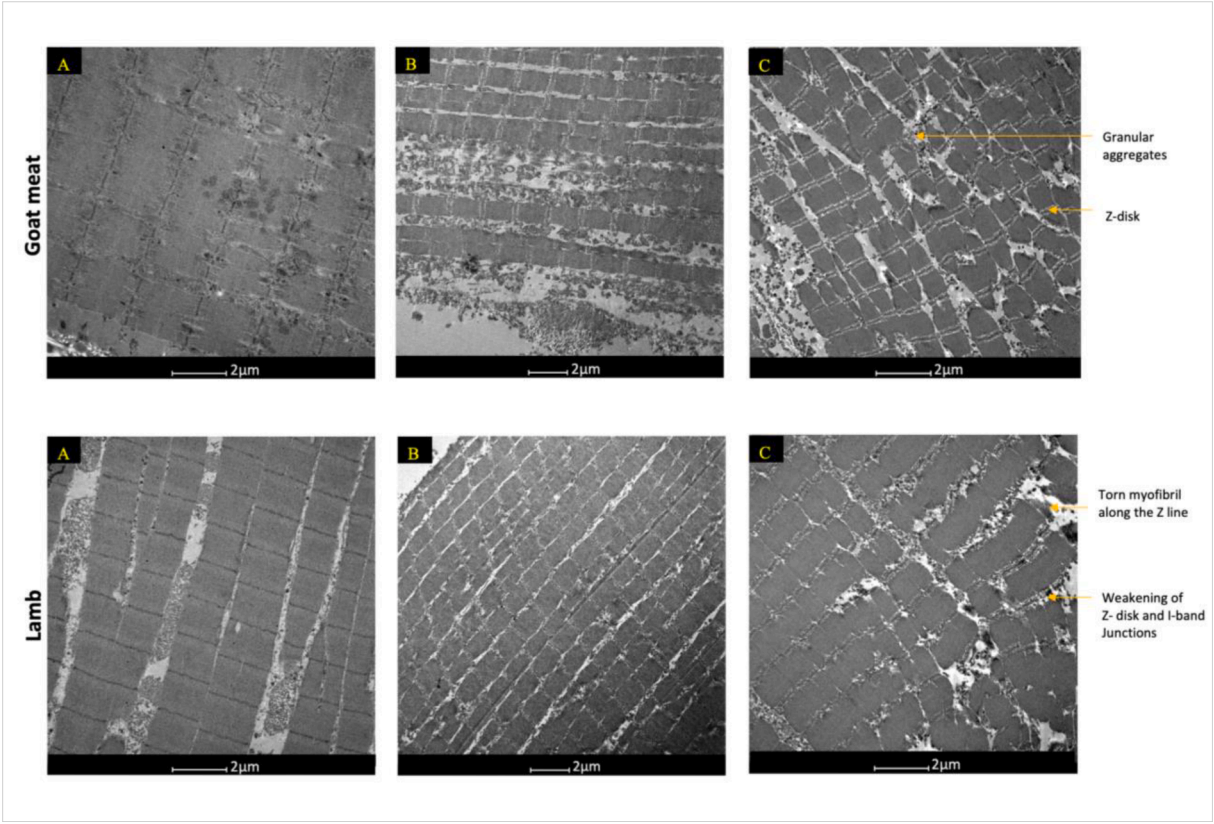

Fig. 1. Meat ultrastructure.Transmission electron microscopy (TEM) images were taken from the longitudinal sections of raw (A), sous vide (B), and microwave (C) processed goat meat and lamb *biceps femoris*.

General changes in muscle ultrastructure after SV and MW also involved the lateral and longitudinal shrinkage of myofibrils as affected by temperature; above 60 °C, shrinkage proceeds, both in diameter and in the longitudinal axis (Dominguez-Hernandez et al., 2018). The shrinkage percentage for the muscle fibers based on TEM images is shown in Supplementary Table 2. For goat meat samples, the longitudinal shrinkage was high. Both processes resulted in a shrinkage higher than 25%, while the transverse shrinkage was just below 20%. Notably, the transverse shrinkage for SV was significantly less compared to the MW samples. Muscle shrinkage occurs because of the significant reduction in muscle fiber diameter if the processing temperature increases from 50 to 60 °C (Tornberg, 2005). MW samples also showed higher longitudinal and lateral shrinkage for lamb, but the transverse shrinkage was higher than the longitudinal shrinkage. The higher transverse shrinkage for lamb can be related to the effect of myofibril integrity for aged meat.

3.3. Myofibrillar protein surface hydrophobicity

Myofibrillar protein surface hydrophobicity results from protein unfolding as the protein structure changes. Our values show that both treatments significantly induced protein unfolding, exposing the hydrophobic side chains of amino acids that bind with BPB (Table 1). Between SV and MW, for both lamb and goat meat, MW induced a higher degree of protein unfolding compared to SV. The MW process resulted in 185 μg and 180 μg hydrophobicity values for lamb and goat meat, which are significantly higher ($p < 0.05$) compared to the hydrophobicity values of SV samples. The results suggest that hydrophobicity is higher with high processing temperatures, consistent with the trend reported in the literature (Chelh et al., 2006; Promeyrat et al., 2010).

The high myofibrillar protein hydrophobicity in MW samples can also be linked to how heat is generated in meat through dielectric

Table 1
Myofibrillar protein hydrophobicity, particle size ($D_{4,3}$ and $D_{3,2}$), specific surface area, and span of raw, microwave (MW), and sous vide (SV) processed lamb and goat meat.

Parameters	Raw		SV	MW
Goat meat				
	Myofibrillar protein hydrophobicity (μg)	13.55 ± 1.78^{a}	157.36 ± 5.95^{b}	179.87 ± 2.01^{c}
	$D_{4,3}$ (μm)	39.03 ± 3.67^{a}	61.35 ± 5.11^{b}	67.83 ± 4.75^{b}
	$D_{3,2}$ (μm)	9.66 ± 0.13^{a}	21.92 ± 1.11^{b}	24.71 ± 1.97^{b}
	Specific surface area (m^2/g)	0.62 ± 0.01^{a}	0.28 ± 0.01^{b}	0.26 ± 0.02^{b}
	Span	6.72 ± 0.36^{a}	3.33 ± 0.39^{b}	3.59 ± 0.10^{b}
Lamb				
	Myofibrillar protein hydrophobicity (μg)	26.37 ± 3.17^{a}	138.49 ± 0.45^{b}	184.52 ± 0.07^{c}
	$D_{4,3}$ (μm)	42.73 ± 2.77^{a}	110.84 ± 5.30^{c}	74.07 ± 4.70^{b}
	$D_{3,2}$ (μm)	9.99 ± 0.45^{a}	28.60 ± 0.97^{c}	22.32 ± 1.45^{b}
	Specific surface area (m^2/g)	0.61 ± 0.03^{a}	0.21 ± 0.00^{b}	0.28 ± 0.02^{b}
	Span	6.82 ± 0.30^{a}	4.09 ± 0.08^{b}	4.68 ± 0.16^{b}

All values are reported as the mean ± SE, where $N = 3$ (3 replicates with three measurements from each replicate).
Values within a row not having common superscripts differ significantly ($p < 0.05$).
MW-microwave process and SV-sous vide process.

heating by MW. In meat proteins, the rupture of hydrogen bonds is cited as the leading cause of increased hydrophobicity (Sante-Lhoutellier et al., 2007). Therefore, the MW process could have resulted in a higher degree of hydrogen bond disruption since the alternating electromagnetic field of a microwave propagates through the polar water molecules within the muscle fiber. Furthermore, the MW electric field could also directly affect myofibrils due to the tearing effect on the protein structure (Cai et al., 2018; Cao et al., 2019).

On the other hand, the lower hydrophobicity values for SV meat can be caused by lower temperatures and prolonged heating conditions (Cao et al., 2019). Protein surface hydrophobicity increases as heating duration increases (Chelh et al., 2006; Promeyrat et al., 2010). However, increased surface hydrophobicity can also cause more extensive bonding and aggregation, and the hydrophobic side chains of denatured proteins

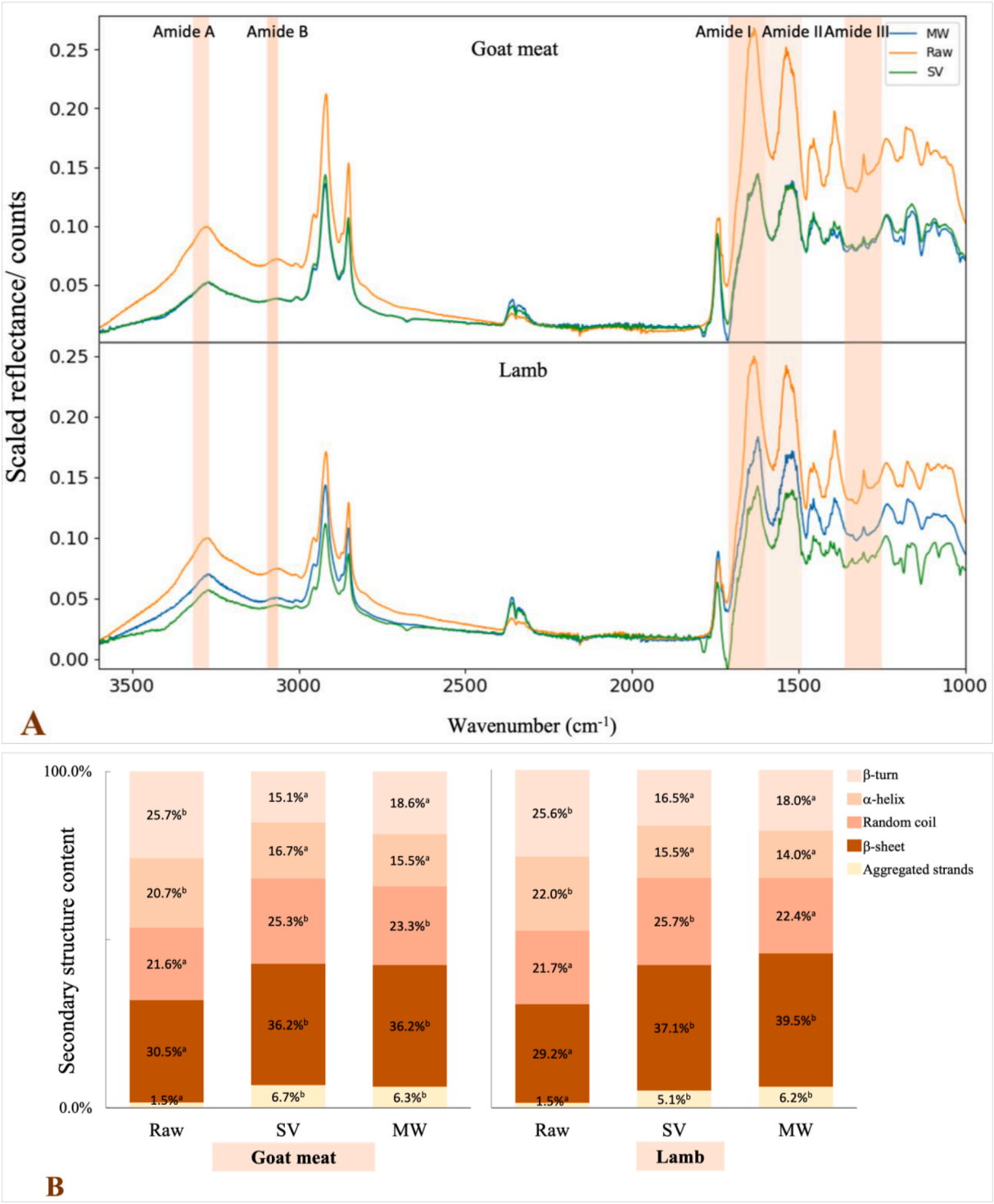

Fig. 2. FTIR spectra (A) and secondary structure content (B) of raw, sous vide (SV), and microwave (MW) goat meat and lamb biceps femoris. Referenced location of secondary structures: Aggregated strands (1610–1620 cm^{-1}), β-sheet (1620–1640 cm^{-1}), Random coil (1643–1650 cm^{-1}), α-helix (1650–1660 cm^{-1}) and β-turn (1660–1695 cm^{-1}) (Barth, 2007; Ngarize et al., 2004). All values are reported as the mean ± SEM, where N = 3 (3 replicates with 3 measurements). Values within a row not having common superscripts differ significantly ($p < 0.05$).

tend to be embedded in clusters when proteins aggregate further, thus reducing the observable surface hydrophobicity.

3.4. Protein degree of aggregation

The volume moment value ($D_{4,3}$) indicates the size of the coarse particulates that comprise the bulk of the isolated myofibrils; this value can provide the degree of myofibrillar aggregation and dissolution (Table 1). Both MW and SV treatments for both meat samples promoted myofibrillar aggregation based on significantly higher ($p < 0.05$) $D_{4,3}$ values than the raw meat samples. Additionally, $D_{3,2}$ was higher ($p < 0.05$) for MW and SV samples compared to raw, signifying a larger size for the fine particulates for MW and SV samples. It was evident that SV and MW temperature was enough to induce significant protein unfolding, which leads to aggregate formation due to the intra or intermolecular cross-linking between unfolded protein molecules, starting at 30 °C (Tornberg, 2005).

Values show that the aggregation mechanisms between the two processing conditions are different. SV induced greater aggregation based on higher $D_{4,3}$ values and lower $D_{3,2}$ values than MW. Although the high temperature has been reported to cause greater unfolding of myosin and rapid formation of larger aggregates (Cao et al., 2019; Promeyrat et al., 2010), the larger aggregates seen for lamb SV than MW can be linked to the effect of heating time. Prolonged heating leads to a higher order of protein aggregation since protein aggregates tend to cluster with time (Cao et al., 2019). This observation was also reported by Mitra et al. (2017), where a high-temperature short-time process had lower $D_{4,3}$ and protein aggregation required a longer cooking time for larger aggregates to form. On the other hand, for the goat meat sample, MW and SV showed no significant differences ($p > 0.05$) for $D_{4,3}$ (61——68 μm) and $D_{3,2}$ (21–25 μm); SV and MW led to the same degree of aggregation. The characteristics of protein aggregation after processing could also depend on the sample type. Other parameters, such as specific surface area and span (width of distribution) of the particulates, were the same for both treatments for both lamb and goat meat samples. The significantly higher ($p < 0.05$) span values for raw meat indicate a more uniform distribution of myofibrils compared to lower span values for SV and MW samples.

3.5. FTIR spectroscopy

FTIR spectra can show qualitative information about protein conformational changes after processing. The FTIR spectra for raw, SV, and MW samples are shown in Fig. 2A, highlighting the major amide bands (amide I, II, III, A, and B); these are characteristic bands present for protein samples. The details of the location and assignment of each peak are in Table 2. Compared to SV and MW, the absorption intensity of overall FTIR spectra of raw samples was higher for both lamb and goat meat. However, after processing, the SV and MW caused a significant shift in peak location for most amide bands. Interestingly, the effect of SV and MW processes on peak location was observed in the lamb sample only; amide A and B for SV lamb had lower wavenumbers. The lower frequency for the amide A and B region for the lamb can be explained by the significant differences in protein aggregation and hydrophobicity between SV and MW lamb, which is related to hydrogen bond formation.

The peak location for the amide I (the most intense absorption band in proteins) shifted from 1634 to 1635 cm^{-1} to 1622–1623 cm^{-1} after SV and MW processing. The lower wavenumber for the processed samples is a characteristic peak of a denatured protein after processing (Ngarize et al., 2004). The exact position of the amide I band results from the backbone conformation and hydrogen bonding characteristics of proteins, which is primarily exhibited by the stretching vibrations of the C═O (70–85%) and C—N groups (10–20%) (Barth, 2007). Amide I is sensitive to the strength and the number of hydrogen bonds, which downshifts the natural frequency of the amide (Lorenz-Fonfria, 2020). The effect of hydrogen bonding can also be observed for amide II vibration, which is very sensitive to hydrogen bonding. Both SV and MW resulted in the same degree of frequency downshift in the amide I and amide II regions for lamb and goat meat.

3.5.1. Secondary structure of proteins in amide I region

The secondary structures, including aggregated strands, α-helix, β-sheet, β-turn, and random coil, were estimated from the amide I region (1600–1700 cm^{-1}) (Fig. 2). The deconvolution of the amide I region provides information about the secondary structure of a protein that describes how protein molecules are coiled and folded in a specific direction relative to the secondary structure of the backbone (Barth, 2007).

Surprisingly, although SV and MW processing differ in their heating mechanisms, both processes showed the same trend in the increase or decrease of the identified secondary structures (Fig. 2B). After SV and MW processing, the secondary structure of lamb and goat meat samples showed a marked increase in β-sheet, random coil, and aggregated strand structure, with a significant reduction in α-helix and β-turns, a common observation for heat-induced protein denaturation in meat (Beattie et al., 2008; Berhe et al., 2014; Ngarize et al., 2004). The decrease in α-helix after MW and SV processing indicates a shift from the tighter and very compact α-helix structure to more spread out β-sheet and random coil structures. MW increases non-organized structure and β-sheet that agrees with the reported trend in the literature (Cai et al., 2018; Calabrò & Magazù, 2014). The increase in the bands of aggregated proteins (1610–1620 cm^{-1}) and random coils (1643–1650 cm^{-1}) after

Table 2
Location and assignment of amide peaks in FTIR spectra.

Region	Peak wavenumber (cm^{-1})						Band Assignment
	Goat meat			Lamb			
	Raw	SV	MW	Raw	SV	MW	
Amide A	3279 ± 0^{b}	3272 ± 0^{a}	3271 ± 0^{a}	3277 ± 0^{c}	3272 ± 0^{a}	3273 ± 1^{b}	3310–3270 cm^{-1} N—H and O—H stretching vibration
Amide B	3065 ± 0^{a}	3068 ± 1^{b}	3069 ± 0^{b}	3065 ± 0^{a}	3066 ± 1^{a}	3071 ± 0^{b}	3060–3090 cm^{-1} the overtone of NH- bending
Amide I	1635 ± 0^{b}	1622 ± 0^{a}	1622 ± 0^{a}	1634 ± 0^{b}	1623 ± 0^{a}	1623 ± 0^{a}	1600–1700 cm^{-1} C═O stretching vibration and minor C—N stretching
Amide II	1538 ± 0^{c}	1522 ± 2^{b}	1520 ± 0^{a}	1538 ± 0^{b}	1523 ± 0^{a}	1522 ± 1^{a}	1500–1600 cm^{-1} C—N stretching and N—H bending
Amide III	1305 ± 0^{a}	1305 ± 0^{a}	1305 ± 0^{a}	1305 ± 0^{a}	1305 ± 0^{a}	1305 ± 0^{a}	1250–1350 in-phase combination of NH bending and CN stretching vibration

The location of the identified peaks is from the reported peaks in the literature (Barth, 2007; Ngarize et al., 2004).
All values are reported as the mean ± SEM, where $N = 3$ (3 replicates with three measurements from each replicate).
Values within a row not having common superscripts differ significantly ($p < 0.05$).
MW-microwave process and SV-Sous vide process.

processing occurs because many proteins preferentially adopt a more random coil conformation, a state with a maximum degree of disorder, in the presence of denaturants or upon heating. The increased β-sheet formation can be associated with a more stabilized secondary structure driven by the increase in protein surface hydrophobicity after the collapse of the α-helix structure.

The comparison between the secondary structure content of SV and MW for goat meat samples showed no significant differences ($p < 0.05$). This observation may be related to the same tenderness values after the treatments. Some researchers have reported a correlation between protein structure and tenderness, specifically for α-helix and β-sheet (Beattie et al., 2008; Beattie et al., 2004; Liu et al., 2019). Additionally, particle size and distribution of MW and SV goat meat are the same (Table 1). It can be assumed that there is only a subtle difference in the secondary structure for the SV and MW goat meat samples.

On the other hand, the secondary structure content of SV and MW-treated lamb resulted in a significantly higher ($p < 0.05$) amount of random coil after the SV process. The trend toward the greater formation of random coils in SV-treated lamb can be directly related to the myofibrillar surface hydrophobicity. Hydrophobic interactions play a dominant role in stabilizing β-sheet conformations (Narayanan & Dias, 2013). Between SV and MW, MW induced significantly higher surface hydrophobicity as discussed (Section 3.3), consistent with a more β-sheet structure for the MW sample and lower random coil compared to SV lamb.

The difference in secondary structure changes was only observed for

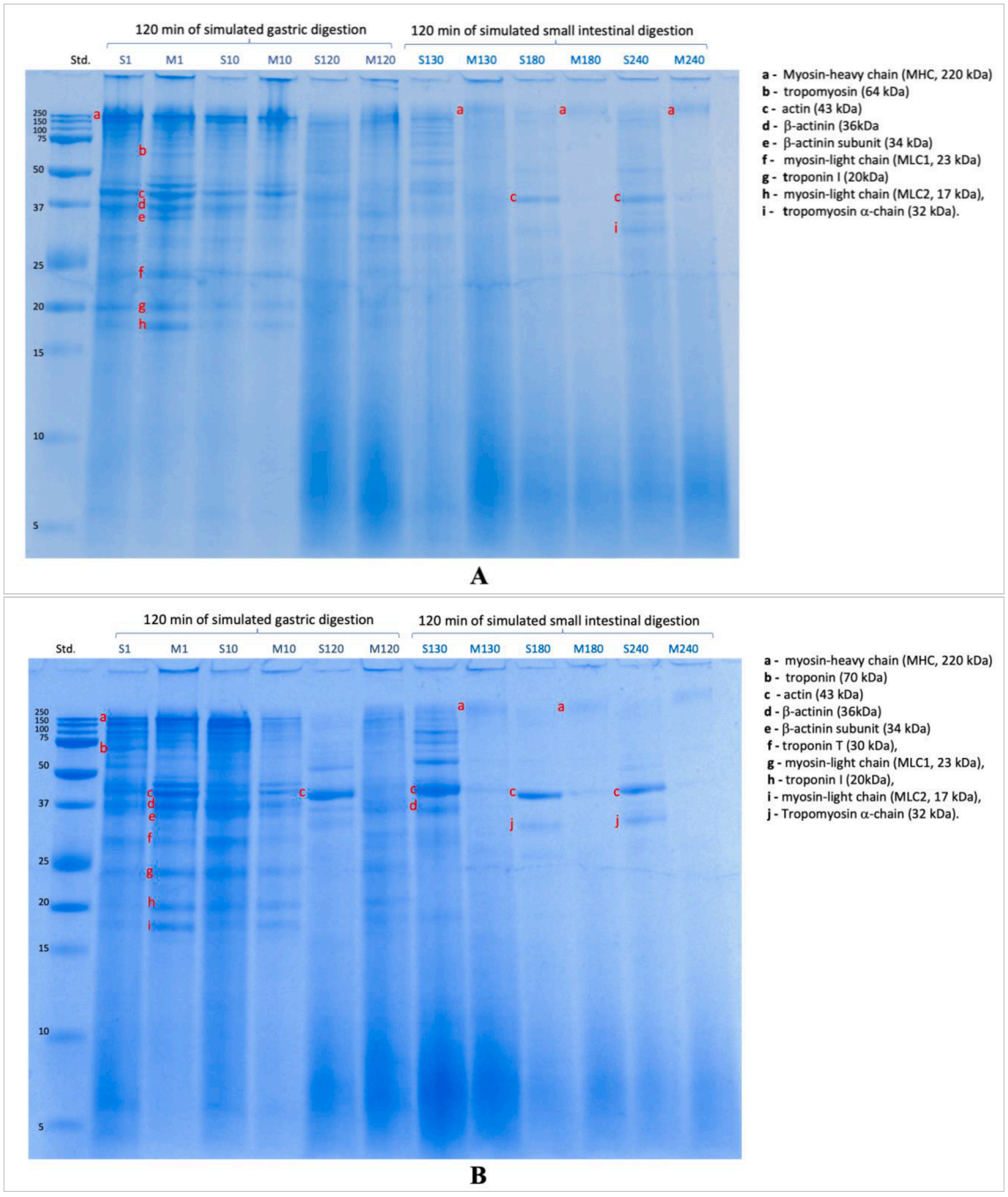

Fig. 3. Tricine SDS-PAGE electrophoretograms of sous vide and microwave goat meat (A) and lamb (B) meat digests after 1, 10, and 120 min of simulated gastric digestion and 130, 180, and 240 min of simulated gastro-small intestinal digestion. S-sous vide and M- microwave for each well in the gel label.

the lamb sample. Although both lamb and goat meat samples are mainly composed of myofibrillar and sarcoplasmic protein, the differences in protein structure and composition and the initial states of the proteins (e.g., more hydrolyzed proteins) will have contributed to the resulting different levels of secondary structure formation when exposed to different thermal processes. The lamb meat proteins, aged longer, have undergone more proteolysis from the endogenous enzyme. Hence its protein structure is more susceptible to denaturation.

3.6. Protein in vitro digestibility

3.6.1. Protein profile of meat digests

The SV and MW process led to a similar pattern of protein breakdown during digestion for both species based on the qualitative data using SDS-PAGE (Fig. 3). After 1 min gastric digestion, MW meat appeared to have a higher degree of protein breakdown; low molecular weight protein (20–23 kDa) already appeared in high intensity compared to the SV sample. These low molecular weight proteins include myosin light chains (20–23 kDa) that are known as the breakdown products of heavy myosin (220 kDa) through enzymatic digestion (Chian et al., 2019). Additionally, the disappearance of β-actinin (130 kDa), α-actinin (95 kDa), proteins that are major components of the Z-disk, showed that these proteins were efficiently hydrolyzed.

As the digestion progressed, bands for actin (43 kDa) and tropomyosin α-chain (32 kDa) were still intense for SV, even at the end of the small-intestinal digestion phase. These bands indicate that these proteins are still in high amounts in the SV meat digest compared to the MW meat sample. On the other hand, the actin band (43 kDa) in MW meat samples was already very faint at the end of digestion. The intense disruption of the Z-disk can explain its efficient breakdown. Since actin is an abundant muscle protein that acts as a structural element of the sarcomere (Obinata et al., 1981), the disruption of the Z-disk shown in TEM images of MW samples would allow pepsin to easily attack these proteins because of their accessibility.

An interesting observation for MW digest is the detectable bands for myosin-heavy chain (MHC, 220 kDa) even at the end of small-intestinal digestion, consistent for both meat samples. Although rapid breakdown of proteins was observed for MW meat samples compared to SV, not all MHC (220 kDa) in MW meat was digested effectively. This high molecular weight protein resisted digestion even after the small-intestinal phase. The gels demonstrate the presence of nonhydrolyzed or partially hydrolyzed proteins at the end of digestion for MW meat samples. The high-temperature MW heating probably resulted in a heterogenous aggregate formation and some of which might be more resistant to digestion, as seen in our gels. It has been reported that MW induced the formation of irregular aggregate clusters (Promeyrat et al., 2010), affecting the digestibility of cooked meat.

The protein digestion pattern of the SV cooked sample shows slow and progressive hydrolysis of peptides as the digestion progress. SV processing might have led to larger but more uniform aggregated myofibrillar proteins that require a longer time to be fully digested. As explained by Bax et al. (2012), more compact protein aggregates have fewer cleavage sites, thus reducing the rate of proteolysis. Only small peptides were visible at the end of the digestion of SV-treated samples.

3.6.2. Degree of protein hydrolysis (Ninhydrin assay)

The results in Table 3 show the degree of protein digestibility as measured by free amino N release for both lamb and goat meat. At the end of gastric digestion, free amino nitrogen values are at varying levels (not significant, $p > 0.05$). This is where the effect of the degree of aggregation can somehow be observed. Since the major action of pepsin is more on breaking down large peptides into small polypeptide chain, the starting structure and size of the sample is important. As the digestion progressed to the small intestinal phase, the values started to level, and the action of pancreatic enzymes was very apparent. There was a significant increase in free amino N after the addition of pancreatin, attributable to pancreatic enzymes being more efficient in hydrolyzing proteins and possibly better solubility of proteins at a neutral pH.

Table 3
In vitro protein digestibility of sous vide (SV) and microwave (MW) samples after 0, 10, and 120 min of simulated gastric digestion and 10, 60, and 120 min of simulated small intestinal digestion. The protein digestibility was measured in terms of ninhydrin-free amino nitrogen released from the collected digest.

Digestion Time (min)		Goat meat		Lamb	
		SV	MW	SV	MW
Simulated gastric digestion	1	3.09 ± 0.17^{a1}	2.35 ± 0.21^{a1}	3.80 ± 0.13^{a1}	2.56 ± 0.10^{a1}
	10	3.19 ± 0.09^{a1}	3.47 ± 0.83^{ab1}	5.19 ± 0.73^{a1}	3.77 ± 0.54^{a1}
	120	3.90 ± 0.38^{a1}	5.08 ± 0.42^{b1}	6.75 ± 0.27^{ab1}	4.44 ± 0.77^{a1}
Simulated small-intestinal digestion	10	8.82 ± 0.44^{b1}	9.12 ± 0.65^{c1}	9.83 ± 0.86^{bc1}	9.15 ± 1.07^{b1}
	60	9.87 ± 0.49^{b1}	10.87 ± 0.12^{c1}	10.88 ± 1.09^{bc1}	10.93 ± 1.05^{b1}
	120	10.33 ± 1.77^{b1}	10.93 ± 0.22^{c1}	13.61 ± 1.65^{c1}	12.48 ± 1.28^{b1}

All values are reported as the mean ± SE, where $N = 3$ (3 replicates with three measurements from each replicate).
[a-c]Values within a column having common superscripts do not differ significantly within species ($p < 0.05$).
[1]Values within a row having common superscripts do not differ significantly within species ($p < 0.05$).

Meat protein digestibility depends on both temperature and time of cooking (Bax et al., 2013). However, our data shows that the varying conditions between SV and MW processing resulted in a non-significant difference ($p < 0.05$) in the overall goat meat and lamb protein digestibility, even though SV and MW resulted in a different pattern of how meat proteins were hydrolyzed (**section 3.6.1**). SV resulted in a larger aggregate size but probably had a less compact structure observed for low-temperature processing (Promeyrat et al., 2010). Also, the structure of proteins for the SV processed meat had more random coils or unordered structures that are less stable and can be slowly attacked by digestive enzymes. On the other hand, MW resulted in aggregates of varying sizes with more stable-sheett and compact structures, some of which became resistant to digestion. The digestive enzymes acted the smaller aggregates easily while the larger aggregates required longer digestion time to be hydrolyzed. SV and MW process then resulted in proteins with a varying structural feature that affects how digestive enzymes can attack the cleavage sites but can still result in the same digestibility.

Furthermore, the same digestibility values between the two processes can be related to the same level of tenderness that resulted in the minimal variation between the secondary structure content of the SV and MW samples (Section 3.5.2). Others have reported that the nutritive value of a protein is also influenced by the secondary structure (Calabrò & Magazù, 2014). In our result, since there is only a minimal difference in secondary structure (only random coil content for the lamb sample), the effect of secondary structure on meat protein digestibility was not seen. The impact of secondary structure content may be apparent only if the difference in the levels of the secondary structure is huge, specifically the content of random coils and β-sheet. It should be noted that the use of free amino N as the basis for the digestibility of protein has limitations, such that it only estimates the level of free amino N but not how polypeptides are degraded to their constituent amino acids. This is a limitation of this study that needs to be clarified using a more extensive method, such as peptidomics.

Meat digestibility also depends on the raw materials and varies within samples. For example, goat and lamb meat samples resulted in varying levels of free amino N at the end of the digestion. SV and MW processed goat meat had digestibility values of 10.3–10.9%, while lamb had digestibility scores of 12.5–13.6%. This difference is probably due to

the varying postmortem conditions of the raw materials before processing. Lamb was aged longer than goat meat, and this could have resulted in greater proteolysis due to endogenous enzyme activity. Consequently, this condition led to a more tender lamb than goat meat. The lesser muscle structure integrity facilitates digestive enzyme bioaccessibility resulting in higher digestibility values for lamb (Astruc, 2014).

3.7. Conclusions

MW cooking can cook lamb and goat meat *biceps femoris* with the same tenderness as meat SV processed at 60 °C for 9 h. However, there was a significant difference in the quality of the cooked samples. The MW process resulted in higher cooking loss which should be addressed when designing pre-packed meals using MW technology. Additionally, MW resulted in a significant reduction of redness and pronounced ultrastructure changes. MW and SV increased surface hydrophobicity and aggregation of the myofibrillar protein. Still, the MW induced higher hydrophobicity than SV, which also drives the formation of more β-sheet, observed in the lamb sample.

Our results imply that even though MW is an intense process (high-temperature process), it does not mean that it can significantly reduce the digestibility of proteins compared to the milder effects of SV cooking at 60 °C. Two extremely different techniques for cooking meat can result in the same digestibility values based on protein hydrolysis, which can be correlated to the same level of tenderness and is also related to the level of protein structural changes. Hence, the resulting secondary structure plays a significant role in the protein digestibility of meat. These results warrant further investigation regarding the relationship between meat protein digestibility as affected by protein structural modification relative to meat tenderness and secondary protein structure. Furthermore, the impact of MW heating can further be investigated, targeting its capacity to modify protein structure and digestibility based on its intensity and repeated microwave exposure.

Funding

This work was supported by the Riddet Institute Centre of Research Excellence and Massey University (School of Food and Advanced Technology), New Zealand.

CRediT authorship contribution statement

Mariero Gawat: Writing – review & editing, Writing – original draft, Data curation, Investigation, Formal analysis, Validation, Software, Methodology, Conceptualization, Methodology, Writing – review & editing. **Mike Boland:** Visualization, Supervision, Resources, Methodology, Writing – review & editing. **Jim Chen:** Methodology, Writing – review & editing. **Jaspreet Singh:** Visualization, Supervision, Methodology, Writing – review & editing. **Lovedeep Kaur:** Project administration, Funding acquisition, Visualization, Supervision, Data curation, Resources, Validation, Methodology, Writing – review & editing, Conceptualization.

Declaration of Competing Interest

The authors declare that they have no known competing financial interests or personal relationships that could have appeared to influence the work reported in this paper.

Data availability

Data will be made available on request.

Acknowledgments

The authors would like to acknowledge the New Zealand Government (Ministry of Foreign Affairs and Trade-NZ Scholarships) for the Ph. D. scholarship grant for Mariero H. Gawat. In addition, sincere thanks are extended to Dr. Mark Waterland of Massey School of Natural Sciences for his valuable time and knowledge for FTIR instrument training and spectral data processing; Marie-Laure Delabre and Raul Cruz of FIET team Massey University for their inputs in the initial stage of the microwave study; Miss Yanyu He of Manawatu Microscopy Imaging Centre for the processing of TEM samples; Mr. Dougal Laidlaw of New Zealand Premium Goat Meat for sourcing goats; Ms. Nicola of Moreish for the use of their butchering facility; and Mr. Simon Wishnowsky of Venison Packers Feilding Ltd. for the use of their slaughtering facility.

Appendix A. Supplementary material

Supplementary data to this article can be found online at https://doi.org/10.1016/j.foodchem.2023.137442.

References

Aoac. (1990). Official Method 984.13. *Official Methods of Analysis of AOAC International* ((15th ed.).). Gaithersburg, MD, USA: AOAC.

Astruc, T. (2014). Muscle structure and digestive enzyme bioaccessibility to intracellular compartments. In M. Boland, M. Golding, & H. Singh (Eds.), *Food Structures, Digestion and Health* (pp. 193–222). Academic Press.

Barth, A. (2007). Infrared spectroscopy of proteins. Biochimica et Biophysica Acta (BBA) -. *Bioenergetics, 1767*(9), 1073–1101. https://doi.org/10.1016/j.bbabio.2007.06.004

Bax, M.-L., Aubry, L., Ferreira, C., Daudin, J.-D., Gatellier, P., Rémond, D., & Santé-Lhoutellier, V. (2012). Cooking Temperature Is a Key Determinant of in Vitro Meat Protein Digestion Rate: Investigation of Underlying Mechanisms. *Journal of Agricultural and Food Chemistry, 60*(10), 2569–2576. https://doi.org/10.1021/jf205280y

Bax, M. L., Sayd, T., Aubry, L., Ferreira, C., Viala, D., Chambon, C., … Santé-Lhoutellier, V. (2013). Muscle composition slightly affects in vitro digestion of aged and cooked meat: Identification of associated proteomic markers. *Food Chemistry, 136*(3), 1249–1262. https://doi.org/10.1016/j.foodchem.2012.09.049

Beattie, J. R., Bell, S. E., Borggaard, C., & Moss, B. W. (2008). Preliminary investigations on the effects of aging and cooking on the Raman spectra of porcine longissimus dorsi. *Meat science, 80*(4), 1205–1211.

Beattie, R. J., Bell, S. J., Farmer, L. J., Moss, B. W., & Patterson, D. (2004). Preliminary investigation of the application of Raman spectroscopy to the prediction of the sensory quality of beef silverside [Article]. *Meat Science, 66*(4), 903–913. https://doi.org/10.1016/j.meatsci.2003.08.012

Berhe, D. T., Engelsen, S. B., Hviid, M. S., & Lametsch, R. (2014). Raman spectroscopic study of effect of the cooking temperature and time on meat proteins. *Food Research International, 66*, 123–131. https://doi.org/10.1016/j.foodres.2014.09.010

Bhat, Z. F., Morton, J. D., Zhang, X., Mason, S. L., & Bekhit, A.-E.-D.-A. (2020). Sous-vide cooking improves the quality and in-vitro digestibility of Semitendinosus from culled dairy cows. *Food Research International, 127*, Article 108708. https://doi.org/10.1016/j.foodres.2019.108708

Brodkorb, A., Egger, L., Alminger, M., Alvito, P., Assunção, R., Ballance, S., … Recio, I. (2019). INFOGEST static in vitro simulation of gastrointestinal food digestion. *Nature Protocols, 14*(4), 991–1014. https://doi.org/10.1038/s41596-018-0119-1

Cai, L., Feng, J., Cao, A., Zhang, Y., Lv, Y., & Li, J. (2018). Denaturation kinetics and aggregation mechanism of the sarcoplasmic and myofibril proteins from grass carp during microwave processing. *Food and Bioprocess Technology, 11*(2), 417–426. https://doi.org/10.1007/s11947-017-2025-x

Calabrò, E., & Magazù, S. (2014). Non-Thermal Effects of Microwave Oven Heating on Ground Beef Meat Studied in the Mid-Infrared Region by Fourier Transform Infrared Spectroscopy. *Spectroscopy Letters, 47*(8), 649–656. https://doi.org/10.1080/00387010.2013.828313

Calabrò, E., & Magazù, S. (2020). Modulation of Maillard reaction and protein aggregation in bovine meat following exposure to microwave heating and possible impact on digestive processes: An FTIR spectroscopy study. *Electromagnetic Biology and Medicine, 39*(2), 129–138. https://doi.org/10.1080/15368378.2020.1737805

Cao, H., Jiao, X., Fan, D., Huang, J., Zhao, J., Yan, B., … Wang, M. (2019). Microwave irradiation promotes aggregation behavior of myosin through conformation changes. *Food Hydrocolloids, 96*, 11–19.

Chelh, I., Gatellier, P., & Santé-Lhoutellier, V. (2006). Technical note: A simplified procedure for myofibril hydrophobicity determination. *Meat Science, 74*(4), 681–683. https://doi.org/10.1016/j.meatsci.2006.05.019

Chian, F. M., Kaur, L., Oey, I., Astruc, T., Hodgkinson, S., & Boland, M. (2019). Effect of Pulsed Electric Fields (PEF) on the ultrastructure and in vitro protein digestibility of bovine longissimus thoracis. *LWT, 103*, 253–259. https://doi.org/10.1016/j.lwt.2019.01.005

Destefanis, G., Brugiapaglia, A., Barge, M. T., & Dal Molin, E. (2008). Relationship between beef consumer tenderness perception and Warner-Bratzler shear force. *Meat Science, 78*(3), 153–156. https://doi.org/10.1016/j.meatsci.2007.05.031

Dominguez-Hernandez, E., Salaseviciene, A., & Ertbjerg, P. (2018). Low-temperature long-time cooking of meat: Eating quality and underlying mechanisms. *Meat Science, 143*, 104–113. https://doi.org/10.1016/j.meatsci.2018.04.032

Dong, X., Wang, J., & Raghavan, V. (2021). Impact of microwave processing on the secondary structure, in-vitro protein digestibility and allergenicity of shrimp (Litopenaeus vannamei) proteins. *Food Chemistry, 337*, Article 127811. https://doi.org/10.1016/j.foodchem.2020.127811

Fellows, A. P., Casford, M. T. L., & Davies, P. B. (2020). Spectral Analysis and Deconvolution of the Amide I Band of Proteins Presenting with High-Frequency Noise and Baseline Shifts. *Applied Spectroscopy, 74*(5), 597–615. https://doi.org/10.1177/0003702819898536

García-Segovia, P., Andrés-Bello, A., & Martínez-Monzó, J. (2007). Effect of cooking method on mechanical properties, color and structure of beef muscle (M. pectoralis). *Journal of Food Engineering, 80*(3), 813–821. https://doi.org/10.1016/j.jfoodeng.2006.07.010

Gawat, M., Kaur, L., Singh, J., & Boland, M. (2022). Physicochemical and quality characteristics of New Zealand goat meat and its ultrastructural features. *Food Research International, 161*, Article 111736. https://doi.org/10.1016/j.foodres.2022.111736

Kaur, L., Rutherfurd, S. M., Moughan, P. J., Drummond, L., & Boland, M. J. (2010). Actinidin Enhances Gastric Protein Digestion As Assessed Using an in Vitro Gastric Digestion Model. *Journal of Agricultural and Food Chemistry, 58*(8), 5068–5073. https://doi.org/10.1021/jf903332a

Liu, H., Wang, Z., Suleman, R., Shen, Q., & Zhang, D. (2019). Effect of protein thermal stability and protein secondary structure on the roasted mutton texture and colour from different cuts. *Meat Science, 156*, 52–58. https://doi.org/10.1016/j.meatsci.2019.05.014

Lorenz-Fonfria, V. A. (2020). Infrared Difference Spectroscopy of Proteins: From Bands to Bonds. *Chemical Reviews, 120*(7), 3466–3576. https://doi.org/10.1021/acs.chemrev.9b00449

Martinaud, A., Mercier, Y., Marinova, P., Tassy, C., Gatellier, P., & Renerre, M. (1997). Comparison of Oxidative Processes on Myofibrillar Proteins from Beef during Maturation and by Different Model Oxidation Systems. *Journal of Agricultural and Food Chemistry, 45*(7), 2481–2487. https://doi.org/10.1021/jf960977g

Mitra, B., Rinnan, Å., & Ruiz-Carrascal, J. (2017). Tracking hydrophobicity state, aggregation behaviour and structural modifications of pork proteins under the influence of assorted heat treatments. *Food Research International, 101*, 266–273. https://doi.org/10.1016/j.foodres.2017.09.027

Moore, S. (1968). Amino acid analysis: Aqueous dimethyl sulfoxide as solvent for the ninhydrin reaction [Article]. *Journal of Biological Chemistry, 243*(23), 6281–6283.

Mortensen, M., Andersen, H. J., Engelsen, S. B., & Bertram, H. C. (2006). Effect of freezing temperature, thawing and cooking rate on water distribution in two pork qualities. *Meat Science, 72*(1), 34–42. https://doi.org/10.1016/j.meatsci.2005.05.027

Narayanan, C., & Dias, C. (2013). Roles of Hydrophobic Interactions and Hydrogen Bonds in Beta-Sheet Formation. *The Journal of chemical physics, 139*, Article 115103. https://doi.org/10.1063/1.4821596

Ngarize, S., Herman, H., Adams, A., & Howell, N. (2004). Comparison of Changes in the Secondary Structure of Unheated, Heated, and High-Pressure-Treated β-Lactoglobulin and Ovalbumin Proteins Using Fourier Transform Raman Spectroscopy and Self-Deconvolution. *Journal of Agricultural and Food Chemistry, 52*(21), 6470–6477. https://doi.org/10.1021/jf030649y

Obinata, T., Maruyama, K., Sugita, H., Kohama, K., & Ebashi, S. (1981). Dynamic aspects of structural proteins in vertebrate skeletal muscle. *Muscle & Nerve: Official Journal of the American Association of Electrodiagnostic Medicine, 4*(6), 456–488.

Promeyrat, A., Bax, M. L., Traoré, S., Aubry, L., Santé-Lhoutellier, V., & Gatellier, P. (2010). Changed dynamics in myofibrillar protein aggregation as a consequence of heating time and temperature. *Meat Science, 85*(4), 625–631. https://doi.org/10.1016/j.meatsci.2010.03.015

Roldán, M., Antequera, T., Martín, A., Mayoral, A. I., & Ruiz, J. (2013). Effect of different temperature-time combinations on physicochemical, microbiological, textural and structural features of sous-vide cooked lamb loins. *Meat Science, 93*(3), 572–578. https://doi.org/10.1016/j.meatsci.2012.11.014

Sante-Lhoutellier, V., Aubry, L., & Gatellier, P. (2007). Effect of Oxidation on In Vitro Digestibility of Skeletal Muscle Myofibrillar Proteins. *Journal of Agricultural and Food Chemistry, 55*(13), 5343–5348. https://doi.org/10.1021/jf070252k

Soni, A., Smith, J., Thompson, A., & Brightwell, G. (2020). Microwave-induced thermal sterilization- A review on history, technical progress, advantages and challenges as compared to the conventional methods. *Trends in Food Science & Technology, 97*, 433–442. https://doi.org/10.1016/j.tifs.2020.01.030

Sun, X., Ohanenye, I. C., Ahmed, T., & Udenigwe, C. C. (2020). Microwave treatment increased protein digestibility of pigeon pea (Cajanus cajan) flour: Elucidation of underlying mechanisms. *Food Chemistry, 329*, Article 127196. https://doi.org/10.1016/j.foodchem.2020.127196

Tornberg, E. (2005). Effects of heat on meat proteins – Implications on structure and quality of meat products. *Meat Science, 70*(3), 493–508. https://doi.org/10.1016/j.meatsci.2004.11.021

Wang, X., Muhoza, B., Wang, X., Feng, T., Xia, S., & Zhang, X. (2019). Comparison between microwave and traditional water bath cooking on saltiness perception, water distribution and microstructure of grass crap meat. *Food Research International, 125*, Article 108521. https://doi.org/10.1016/j.foodres.2019.108521

Xiang, S., Zou, H., Liu, Y., & Ruan, R. (2020). Effects of microwave heating on the protein structure, digestion properties and Maillard products of gluten. *Journal of Food Science and Technology, 57*(6), 2139–2149. https://doi.org/10.1007/s13197-020-04249-0